Published in final edited form as:
Virology. 2014 March ; 0: 202–211. doi:10.1016/j.virol.2014.01.017.

Improved genetic stability of recombinant yellow fever 17D virus expressing a lentiviral Gag gene fragment

Marlon G. Veloso de Santana[1,3,*], **Patrícia C.C. Neves**[1,*], **Juliana Ribeiro dos Santos**[1], **Noemia S. Lima**[1], **Alexandre A. C. dos Santos**[1], **David I. Watkins**[3], **Ricardo Galler**[2], and **Myrna C. Bonaldo**[1,**]

[1]Laboratório de Biologia Molecular de Flavivírus, Instituto Oswaldo Cruz, FIOCRUZ, Rio de Janeiro, Brazil

[2]Instituto de Tecnologia em Imunobiológicos, Fundação Oswaldo Cruz, Rio de Janeiro, Brazil

[3]Department of Pathology, University of Miami, Miller School of Medicine, United States of America

Abstract

We have previously designed a method to construct viable recombinant Yellow Fever (YF) 17D viruses expressing heterologous polypeptides including part of the Simian Immunodeficiency Virus (SIV) Gag protein. However, the expressed region, encompassing amino acid residues from 45 to 269, was genetically unstable. In this study, we improved the genetic stability of this recombinant YF 17D virus by introducing mutations in the IRES element localized at the 5′ end of the SIV gag gene. The new stable recombinant virus elicited adaptive immune responses similar to those induced by the original recombinant virus. It is, therefore, possible to increase recombinant stability by removing functional motifs from the insert that may have deleterious effects on recombinant YF viral fitness.

Keywords

Yellow Fever 17D virus; viral vector; genetic stability; SIV *gag* IRES; SIV Gag; recombinant virus

Introduction

Yellow Fever (YF) 17D is one of the most effective vaccines currently available. It was developed by Max Theiler and associates, who attenuated wild type strain Asibi by serial passages in animal tissues. This vaccine has been used for 75 years in more than 540 million

**Corresponding author: Myrna C. Bonaldo, Lab. Biologia Molecular de Flavivírus, Instituto Oswaldo Cruz – FIOCRUZ, Pav. Leônidas Deane, sala 317, Av. Brasil, 4365 – Manguinhos, Rio de Janeiro, RJ, Brasil, CEP 21040-900, mbonaldo@ioc.fiocruz.br, myrna.bonaldo@gmail.com, tel: 55 21 3865 8112, fax: 55 21 3865 8200.
*These authors contributed equally to this work.

Competing interests.
The author(s) have declared that the present methodology to obtain recombinant SIV/HIV YF viruses is the subject of a patent application having as authors MCB, RG and DIW and the Fundação Oswaldo Cruz as well as the University of Miami as the sponsoring institutions.

people with an outstanding record of efficacy and safety. A single subcutaneous injection confers protection for at least 10 years (Ciczora et al., 2010; Monath, 2004). The basis of this strong and durable immune response is currently being investigated. It is known that this vaccine virus activates different pathways of the innate immune response, which lead to a polyvalent adaptive response. Vaccination induces cytotoxic CD8+ T memory cells, neutralizing antibody production and a mixed T_H1/T_H2 response (Barba-Spaeth et al., 2005; Miller et al., 2005; Querec et al., 2006; Santos et al., 2008).

These exceptional properties of the attenuated YF 17D vaccine have led to the idea that this virus could be used as a vector for the generation of new human vaccines (Bonaldo et al., 2000; Pugachev et al., 2005). The YF virus is the prototype member of the genus Flavivirus, which contains a positive strand RNA genome of about 11 kb (Chambers et al., 1990). Recombinant virus recovery is possible by modifying the complete cDNA infectious clone of the YF 17D vaccine virus, *in vitro* transcription and transfection of infectious RNA molecules.

So far, several strategies have been developed to insert gene sequences encoding microbial antigens in the YF genome. In some of these approaches, short sequences that encode epitopes were inserted into different genomic regions (Barba-Spaeth et al., 2005; Bonaldo et al., 2002; Bonaldo et al., 2005; McAllister et al., 2000; Tao et al., 2005). However, a major concern in the development of recombinant YF 17D vaccines relates to the limited size of the insert, because, unfortunately, inserts longer than 40 codons do not generally produce genetically stable viruses. The expression of larger fragments would be desirable to promote a broader immune response. Hence, we have developed a methodology to construct viable and immunogenic recombinant YF 17D viruses that used the presence of functional motifs and amino acid sequence conservation flanking the E and NS1 intergenic region. Duplication of these sequences and fusion to the exogenous gene facilitated the correct processing of the viral polyprotein precursor (Bonaldo et al., 2007). Using this strategy, we recovered a viable and immunogenic recombinant YF 17D virus expressing a fragment of the SIV Gag protein (residues 45 to 269), which elicited SIV-specific CD8+ T cell responses after immunization of rhesus macaques (Bonaldo et al., 2010). However, this recombinant virus was not stable, resulting in insert loss after serial passages in Vero cell culture. Interestingly, this *gag* 45-269 minigene contains part of a lentiviral IRES motif (Weill et al., 2010). We hypothesized that the IRES motif might cause a substantial reduction in viral fitness leading to the positive selection of recombinant viruses in which the *gag* gene insert has been partially deleted. To explore this hypothesis and create new approaches to overcome this limitation, we constructed a variant recombinant YF 17D virus in which the IRES element was knocked out. The resulting mutant virus retained the foreign cassette for higher numbers of passages when compared to the original recombinant YF17D/SIV $Gag_{45\text{-}269}$ virus. It also retained its biological and immunological properties, providing the basis for further development of this platform for expressing relevant SIV/HIV antigens and the development of new HIV vaccine candidates.

Results and Discussion

Design of SIV *gag* minigene expression cassettes and recombinant YF 17D virus recovery

We have previously described a strategy for the insertion and expression of the heterologous sequences in the YF genomic E/NS1 intergenic region (Bonaldo et al., 2007). The rationale for this approach was based on the fact that this insertion site represents a functional shift from the structural to non-structural flavivirus genes accommodating larger inserts better than any other site in the YF 17D virus genome. In our first attempt to establish the use of the YF 17D virus as a vector to express lentiviral antigens, we inserted the SIV *gag* 45-269 gene region at the YF 17D E-NS1 site (SIVmac239 *gag* gene position: 133-807; GenBank,

AY588945). This SIV gene region corresponds to the last 273 nucleotides of the p17 Matrix protein gene (coding for 91 amino acid residues of the carboxyl-terminus of the Matrix protein) and 402 nucleotides of the 5′ end of the Capsid gene (p24) encoding its first 134 amino acids.

The choice of this SIV antigen was based on the presence of a well-characterized SIVmac239 CD8+ T cell epitope recognized by rhesus monkey T cells (Allen et al., 2001). Recombinant YF17D/SIV viruses could therefore be evaluated for immunogenicity and safety in the rhesus monkey model. Accordingly, we demonstrated that the recombinant YF17D/SIV $Gag_{45\text{-}269}$ virus elicited SIV-specific CD8+ T cell responses in the Indian rhesus macaques after immunization (Bonaldo et al., 2010).

The second criterion for the rational design of the recombinant virus was the physical chemical properties of this SIV $Gag_{45\text{-}269}$ antigen. We also investigated whether the insert encoded any transmembrane domains and whether it was hydrophobic. Both characteristics might be deleterious to the correct topology and processing of the downstream YF polyprotein precursor. The selected SIV $Gag_{45\text{-}269}$ expression cassette encoded 308 amino acids, which included 10 residues from the N-terminus of the YF 17D virus NS1 protein (YF genome position from 2453 to 2482) fused at its 5′ terminal (Figure 1A). At the C-terminal, the $Gag_{45\text{-}269}$ cassette contains the motif KESSIG (YF genomic position from 2145 to 2164) followed by the truncated stem anchor domain of dengue 4 (DENV4) virus E protein containing two transmembrane helix motifs called TM1 and TM2 (DENV4 genome positions 2226 to 2423; GenBank GU289913) (Figure 1A). Both transmembrane domains could be predicted by TMHMM software, specific for transmembrane helices in proteins (Figure 1B). The presence of these transmembrane motifs in the recombinant protein promotes its anchoring in the ER membrane, facing the ER lumen (Bonaldo et al., 2007). Additionally with the ProtParam Tool, we also determined various physicochemical properties, such as the expected molecular weight of 33.7 kDa and its hydrophilic character based on its Grand average of hydropathicity (GRAVY's index) of − 0.138 (Supplementary Table 1). The hydrophilicity of the foreign protein is probably an important property of the recombinant protein, since it should be soluble and exposed in the lumen of ER thereby not disturbing the arrangement of the flanking viral E and NS1 proteins.

Finally, the selected sequence was codon-optimized, based on YF virus codon usage frequency. The synthetic gene was cloned into YF genomic cDNA, which in turn was submitted to *in vitro* transcription. Following Vero cell transfection with RNA, we recovered the recombinant YF virus, identified as YF17D/SIV $Gag_{45\text{-}269}$ virus and re-infected Vero cell monolayers generating a second passage viral stock, called P2, with a viral titer of 6.2 $\log_{10}$ PFU/ml.

The recombinant YF17D/SIV $Gag_{45\text{-}269}$ virus is genetically unstable

Genetic stability is one of the most important properties of a recombinant live attenuated virus for a vaccine candidate. We, therefore, genetically characterized the recombinant YF17D/SIV $Gag_{45\text{-}269}$ virus by sequencing the whole genome to confirm the expected nucleotide sequence of this virus as well as the integrity of the heterologous cassette under successive passages in Vero cells. We did not detect any point mutations in the second passage virus samples (P2). However, by analyzing the size of the RT-PCR amplicons containing the heterologous insertion, we observed a reduction of the cassette size after the fifth Vero cell serial passage (Supplementary Figure 1B). At the twentieth continuous cell passage, most of the amplicons contained only recombinant Gag sequence of the first 27 nucleotides at the 5′ end and the last 178 nucleotides of the $gag_{45\text{-}269}$ gene. We reasoned that the particular region from nucleotide 57 through 528 of the expression cassette might be

deleterious to the virus, and therefore, recombinant YF 17D viruses with smaller foreign inserts were positively selected.

With the aim of understanding the nature of this constraint, we compared the recombinant YF17D/SIV Gag_{45-269} virus to six other recombinant YF 17D viruses expressing SIV Gag regions that were 41 to 166 amino acid residues long (Supplementary Table 2). By comparing the genetic stability based on the amplicon profiles of the complete set of YF17D/SIV Gag viruses, we observed that the most unstable viruses were those expressing Gag_{45-269} and Gag_{76-123} regions (Figure 2). These YF17D/SIV Gag_{45-269} and YF17D/SIV Gag_{76-123} viruses also displayed the lowest growth rates in Vero cells (Supplementary Figure 2). Interestingly, these unstable viruses originally carried part of an Internal Ribosomal Entry Site (IRES) domain present in the *gag* gene sequence that was partially deleted upon serial passage.

Overcoming genetic instability of the *gag* gene expressed by the recombinant YF 17D virus

The primate lentivirus *gag* coding region assumes a stable secondary structure and carries one or several IRES domains that are involved in recruiting the initiation complexes on several initiation codons (Buck et al., 2001; Herbreteau et al., 2005; Nicholson et al., 2006; Weill et al., 2010). In the SIVmac251 genomic RNA, the *gag* gene exhibits three initiation AUG codons and eight intra-molecular base-pairing interactions, P1 to P8. Notably, both *gag* 45-269 and *gag* 76-123 gene fragments bear the pairings P5, P6 and P7, including the translation initiation AUG codon present in P7 (Figure 3A). So, given that the YF17D/SIV Gag_{45-269} and YF17D/SIV Gag_{76-123} viruses are very unstable, we anticipated that these structural and functional IRES motifs might cause a deleterious effect on YF viral fitness disturbing flaviviral translational or replicative processes during cell infection. Accordingly, the creation of bicistronic flaviviruses by inserting sequences corresponding to IRES followed by reporter genes at the 3′ UTR of viral genome generated very unstable viruses leading to a complete deletion of the heterologous IRES-bearing region after few rounds of viral infection cycles (Deas et al., 2005; Pierson et al., 2005; Zou et al., 2011). Therefore, we deduced that mutations disrupting these elements (Figure 3B, C) might improve the genetic stability of the recombinant YF 17D viruses expressing this Gag region.

For this purpose, we selected motifs involved in intra-strand base pairing of stem loop regions of the P6 and P7 elements which corresponds to one of the translation initiation regions based on the secondary structure model described by Weill and coworkers (2010) for the SIVmac251 *gag* 5′ terminal region. In the P6 pairing region, CACC forms a stem with GGUG corresponding to the SIV *gag* gene position from 319 to 322 and 327 to 330, respectively (GenBank AY588946). Despite the fact that the original YF17D/SIV Gag_{45-269} virus bears the CAUC motif instead of CACC, due to the codon optimization synthesis of the *gag* 45-269 minigene sequence, it is well known that uracil and guanine can form a single hydrogen bond base pair in this kind of secondary RNA structure. Thus, codon optimization at this site might not interfere with pair formation in P6. To disrupt the pairing at P6, we modified the GGUGGU sequence present in the recombinant YF17D/SIV Gag_{45-269} virus (SIV *gag* gene position from 324 to 330; GenBank AY588946) to AGUAGUA, without altering any amino acid in the Gag protein fragment. In a second round of mutations, the AUGCC sequence of the P7 motif was mutated to AUCGG (SIV *gag* gene position from 352 to 357). These mutations led to two amino acid modifications, in the first codon, methionine to isoleucine (Gag position 118) and in the second, proline to glycine (Gag position 119). Nevertheless, both cassettes retained the same physicochemical properties, indicating that most probably they would not interfere with structural characteristics (Supplementary Table 1). Furthermore, the amino acid changes did not

disrupt any of the well-characterized SIVmac239 CD8+ and CD4+ T cell epitopes recognized by the immune system of rhesus monkeys and present in the Gag 45-269 fragment (Loffredo et al., 2007) (Supplementary Table 3). The recovered new virus carrying all these mutations was viable and was designated YF17D/SIV GagΔIRES.

Genetic stability and growth properties of the YF17D/SIV $Gag_{45\text{-}269}$ and YF17D/SIV GagΔIRES viruses

In order to access the genetic stability of the new YF17D/SIV GagΔIRES virus, we analyzed amplicons containing the insertion region from viral RNA samples of two independent experiments up to twenty serial passages in Vero cells. In all samples the complete amplicon size of about 1.6 kb was detected without any sign of continuous deletions in the heterologous cassette up to twenty serial passages (Figure 4A). The gain in genetic stability was further confirmed by sequencing the complete YF17D/SIV GagΔIRES genome from the twentieth serial passage samples. We detected neither any point mutation in the heterologous gene nor in the YF genome, indicating that this new recombinant virus is stable.

Despite the increase in genetic stability, the proliferation capability of the YF17D/SIV GagΔIRES virus in Vero cells did not improve when compared to the original YF17D/SIV $Gag_{45\text{-}269}$ virus (Figure 4B). Both recombinant viruses demonstrated lower proliferation rates in comparison with the YF 17D control viruses. This is not surprising, since the insertion of heterologous sequences into the YF genome, in general, led to decreased yields and over attenuation (Bonaldo et al., 2005; Bonaldo et al., 2007; Nogueira et al., 2013). The reduction in yields can be best witnessed at 72 hr post-infection, when the control YF 17DD and YF17D/G1/2T3 viruses peaked with titers of 7.2 ± 0.7 $\log_{10}$ PFU/ml and 7.9 ± 0.5 $\log_{10}$ PFU/ml, respectively, whereas the recombinant YF17D/SIV $Gag_{45\text{-}269}$ exhibited a titer of 6.8 ± 0.2 $\log_{10}$ PFU/ml and YF17D/SIV GagΔIRES of 6.9 ± 0.3 $\log_{10}$ PFU/ml.

The only statistically significant difference in viral growth (*t*-test; $P = 0{,}0003$) between the mutated YF17D/SIV GagΔIRES (6.4 ± 0.1 $\log_{10}$PFU/ml) and the original YF17D/SIV $Gag_{45\text{-}269}$ (5.8 ± 0.1 $\log_{10}$PFU/ml) viruses was detected at 48 hr post-infection.

Expression of YF 17D and Gag proteins in infected Vero cells

When we performed a comparative immunofluorescence assay with a monoclonal antibody against the SIV Capsid p27 protein, the recombinant Gag labeling was mainly localized in the perinuclear region of the cells, (Figure 5A, B) as we expected. This suggested that the recombinant protein was associated with the ER compartment, as previously described for other recombinant viruses, bearing insertions at the E/NS1 site (Bonaldo et al., 2007; Nogueira et al., 2013; Trindade et al., 2012). Indeed, recent studies have revealed that ER maintenance signals are present in the flaviviral E protein and that the length and some non-hydrophobic residues existing in the two transmembrane domains are critical for ER retention (Ciczora et al., 2010; Hsieh et al., 2010). Considering that the recombinant $Gag_{45\text{-}269}$ is a chimeric protein that carries both transmembrane domains in its C-terminal, and consequently their retention motifs, the ER location is conceivable.

In a second set of experiments we characterized the viral protein expression in infected Vero cell monolayers with Western Blotting analysis to establish if the presence of these secondary structured elements could interfere with the synthesis of YF proteins (Figure 5C). Because of the presence of IRES elements mentioned above that could act as a second point of recruitment of factors involved in translation, the synthesis of YF proteins could be altered. However, the relative intensity of YF protein bands corresponding to prM, which is translated from the YF RNA 5′ end and non-structural proteins (NS1 and NS3) located downstream of the secondary-structured *gag* IRES elements, did not differ between the two

recombinant viruses, as evidenced when the two *gag* minigene-containing viruses and the original YF 17D vaccine virus are compared. These data suggested that there were no differences in the translation of the YF genome in terms of the location of YF genes regarding the *gag* gene. As a result, we hypothesized that the deleterious effect associated with the existence of part of a lentiviral *gag* IRES domain could be due to the interaction of the IRES sequence motifs with YF virus RNA folding sequence elements disrupting the original folding (Friebe and Harris, 2010; Gebhard et al., 2011). Alternatively the IRES folding may simply be a signal for the viral polymerase to jump over upon RNA replication, leading to a deleterious effect in the recombinant virus genome.

Immunogenicity of recombinant YF 17D viruses in mice

In the next step of this work, we determined if the genetic modifications of the YF17D/SIV GagΔIRES virus did not impair its ability to promote a proper antibody and cellular immune response against the YF 17D virus and the SIV $Gag_{45\text{-}269}$ foreign antigen. Therefore, BALB/c mice were immunized subcutaneously with two doses of recombinant virus as well as the YF 17DD vaccine counterpart as a positive control and diluent medium as a negative control (mock). In the first study, we evaluated the ability of the recombinant YF 17D viruses to elicit YF virus neutralizing antibodies (Table 1). Both recombinant viruses induced YF neutralizing antibodies in comparison with the mock immunized group ($P < 0.0001$), but the neutralizing antibody titers of the recombinant viruses (YF17D/SIV $Gag_{45\text{-}269}$ - GMT 30 ± 6 and YF17D/SIV GagΔIRES - GMT 30 ± 14) were significantly lower than those for YF 17DD-immunized mice (GMT 182 ± 49; Table 1). This suggested that there was a decrease in immunogenicity induced by the recombinant YF virus, consistent with our previous results with other recombinant viruses (Bonaldo et al., 2007). This, in part, may be due to a reduction in viral fitness, as shown in the growth curves of the recombinant viruses which exhibited a decrease of around 1 $\log_{10}$ PFU/ml at the peak of replication, when compared to the vaccine counterpart YF 17DD. This might lead to limited viral antigen production due to lower infectiousness to the mammalian host. Genetic mutations, resulting from insertion of foreign sequences, could alter viral attenuation and viral viability leading to reduced immunogenicity.

In a second study, we evaluated the cellular immune response against YF and Gag antigens by analyzing IFN-γ production by mouse splenocytes (Figure 6) fifteen days after the second dose. With regard to YF immune response, there was a significant number of IFN-γ spot-forming cells (SFC) against YF in all virus immunized mouse groups in relation to the mock-immunized group. Indeed, the differences in the number of IFN-γ secreting splenocytes among the three virus groups were not significant, with values of 122 ± 21 SFC for YF 17DD, 115 ± 35 SFC for YF17D/SIV $Gag_{45\text{-}269}$ and 139 ± 30 SFC for YF17D/SIV GagΔIRES viruses (Figure 6A). We, therefore, concluded that YF 17D recombinant viruses expressing Gag are equally immunogenic to the commercial YF 17D vaccine virus with regard to their capacity to elicit specific T cells against the YF virus.

Induction of Gag-specific IFN-γ secreting murine splenocytes was equivalent among the two recombinant YF17D/SIV $Gag_{45\text{-}269}$ and YF17D/SIV GagΔIRES viruses (Figure 6B). These responses were significantly higher in groups immunized with recombinant viruses in comparison to the groups immunized with the medium (mock) or YF 17DD virus (Kruskall Wallis test with Dunn's post-test; $P \leq 0.05$) (Figure 6B). In contrast the magnitude of cellular responses elicited by the recombinant viruses was not significantly different. Interestingly, the mutations introduced in the *gag* gene did not change the cellular immune response against Gag. For further insight in this matter, we performed an analysis adopting the IEDB Analysis Resource (http://tools.immuneepitope.org/). We utilized amino acid sequences from both recombinant Gag viruses to predict epitope binding to MHC class I and

II molecules expressed by BALB/c mice (Supplementary Table 4). The predicted epitopes obtained for BALB/c mice were exactly the same for both recombinant viruses and correspond to Gag peptide pools B and E employed in our ELISpot assays. Importantly, these epitopes do not overlap with the mutagenized amino acid positions that are localized in peptide pool C.

Aiming to better characterize the profile of the cellular immune responses induced by YF 17D virus vaccination, we analyzed production of IFN-γ and IL-2 by splenocytes stimulated with whole inactivated YF 17D virus or a peptide pool spanning the Gag_{45-269} protein. This inactivated virus is constituted by YFV structural proteins, which have already been described as having epitopes recognized by MHCs class I and II of BALB/c mice (Maciel et al., 2008).

In this investigation, we initially gated the lymphocytes from splenocyte samples according to cell morphology (FSC x SSC) and to the expression of CD4 or CD8 markers (Supplementary Figure 3). As can be seen in Figure 7 (panels A and C), we detected double positive IL-2+IFN-γ+ lymphocytes in all mouse groups that were immunized with the recombinant viruses and the control YF 17D virus when stimulated by the inactivated YF 17D virus. This phenotype was mainly associated with the CD4+ T cell subset, which was described to be an important feature of immunization with the YF vector (Franco et al., 2010; Neves et al., 2010). The same profile was apparent in CD4+ and CD8+ T cells stimulated with a Gag peptide pool (Fig 7, B and D) in splenocytes from groups immunized with either of the recombinant YF 17D viruses.

Interestingly, despite the genetic modifications performed in the recombinant *gag* gene that promoted a substantial increment in viral genetic stability, these changes did not lead to an increase of viral immunogenicity and proliferation rates. One of the possible explanations could be that the accumulation of the recombinant Gag proteins inside the ER, perhaps forming oligomers due to the presence of part of the SIV capsid protein, could trigger and accelerate cellular stress, leading to a signaling cascade and apoptosis (Todd et al., 2008). In fact, Vero cells infected with the recombinant YF17D/SIV Gag_{45-269} viruses appeared to have accelerated death when compared to the parental virus due to extensive cell mortality early in infection (data not shown). It is known that dendritic cells (DC) engulf apoptotic bodies and present the antigens to CD4+ T cells (Green et al., 2009), and the YF 17D virus infects mouse DC as well as human DCs (Barba-Spaeth et al., 2005; Castellino and Germain, 2006; Palmer et al., 2007; Querec et al., 2006). We, therefore, reasoned that *in vivo* death of infected DCs activates bystander DCs, which might present the YF and Gag epitopes to CD4+ T cells leading to robust CD8 responses, a hallmark of immunization with the YF 17D virus (Castellino and Germain, 2006; Miller et al., 2005). In this regard, it is noteworthy that this same recombinant virus elicited CD8+ T cell responses against Gag epitopes in vaccinated rhesus monkeys (Bonaldo et al., 2010).

Conclusions and Perspectives

In this work we were successful in improving the genetic stability of YF 17D recombinant viruses expressing the SIVmac239 Gag_{45-269} protein fragment by mutating secondary structures present in this gene segment. Importantly, these modifications of the recombinant YF17D/SIV Gag_{45-269} virus were not accompanied by impairments in rates of viral growth or immunogenicity in a mouse model. Accordingly, we are extending these analyses to other YF 17D viruses expressing lentiviral Gag, Nef and Vif fragments. This should provide a better evaluation of immunological properties of the recombinant YF 17D viruses in the development of new HIV vaccine candidates. Obviously, this approach does not apply to other IRES-free sequences and indeed it strongly suggests that to solve the problem of

genetic instability of YF 17D recombinant viruses bearing insertions at E-NS1, we should take into account the functional and structural characteristics of each foreign sequence to be expressed.

Materials and Methods

Cell culture

Vero cells (ATCC) derived from the kidney of an African green monkey were maintained in Earle's 199 complete medium supplemented with 5% fetal bovine serum (FBS).

Generation of recombinant YF 17D/Gag viruses

In the recovery of the YF 17D virus from cDNA, the parental YF17D/G1/2-T3 vector virus and the recombinant YF17D/SIV $Gag_{45\text{-}269}$ virus were constructed employing the two plasmid- infectious clone technology (Rice et al., 1989). In this approach, the entire YF genomic cDNA is split in the pG1/2 and pT3, which are derivatives of the original pYF5′3′IV and pYFM5.2 plasmids (Rice et al., 1989). Plasmid pG1/2, with 6,905 bp contains the first 2,271 nucleotides fused to the 2,588 nucleotides of the 3′ terminal of the YF genome. This plasmid carries the following mutations at the following genomic positions: 1140, 1436/1437, 8808 and 9605 (all displaying amino acid changes) and 10454 and 10722, rendering it 17DD-like (GenBank accession number: U17066.1). Plasmid pT3 is a derivative of pYFM5.2 with 9,939 bp and contains the central portion of the YF genome extended to the SalI site at position 8060 as compared to plasmid pYFM5.2. The T3 plasmid also includes mutations at nucleotides 2356, 2602, 2677, 2681, 8656 (*BstE II* site) and 8808 (Display amino acid changes), as compared to YF 17D-204 (GenBank accession number: X15062.1). The sequences of the inserts were codon-optimized and synthesized by Geneart GmbH (Regensburg, Germany) and then cloned into the pT3 backbone with the EagI/NarI sites. The viral cDNA template was created as well as recombinant viruses obtained as described elsewhere (Bonaldo et al., 2007; Nogueira et al., 2013).

Genetic stability studies and nucleotide sequencing

To access the genetic stability of recombinant YF 17D viruses, two independent serial passage experiments were performed for each recombinant virus. Recombinant viruses were submitted to either fifteen or twenty consecutive passages in Vero cells at a MOI of 0.02. RNA samples of each passage were obtained and sequenced as described elsewhere (Bonaldo et al., 2007). Briefly, viral RNA was extracted from culture supernatants with the QIAamp Viral RNA kit (Qiagen) and amplified by RT-PCR the viral E-NS1 genomic region with a negative strand YF-specific synthetic oligonucleotide (genome position 2772-2795) together with the positive YF-specific primer (genome position 2122-2145). To obtain the sequence of the entire YF genome, a total of 12 RT/PCR products were synthesized encompassing nucleotides 1–1202, 854–2093, 1842–3206, 2871–4261, 3868–5202, 4831–6215, 5873–7195, 6846–8252, 7854–9228, 8850–10195, 9879–10326 and 10230–10862. RT-PCR was carried out with Superscript III (Invitrogen) and GoTaq Green Master Mix (Promega) as recommended by producers. To sequence serial passage samples from the YF17D/SIV $Gag_{45\text{-}269}$ virus that showed a mixed profile of amplicons in the insert region, they were cloned in the pGEM T-Easy plasmid (Promega) and the primers M13F and M13R used to determine the amplicon sequence. All the samples were sequenced by the Sanger sequencing method as previously described (Bonaldo et al., 2007).

Immunofluorescence microscopy

The immunofluorescence analyses were performed as described previously (Bonaldo et al., 2007). The primary mouse α-p27 antibody FITC conjugated (AIDS Research and Reference

Reagent Program, Division of AIDS, NIAID, NIH: SIVmac p27 Hybridoma -55-2F12- from Dr Niels Pedersen) was diluted 1:50 and the antibody mouse α-E protein (clone 2D12, Bio-Manguinhos) was diluted 1:200. For E protein staining, a secondary antibody was used in the analysis diluted 1:400 (Alexa Fluor 546 goat anti-mouse IgG -Invitrogen). Both preparations were treated with SlowFade-Gold antifade reagent with DAPI (Invitrogen, Grand Island, NY) and Fluorescence Microscopy was performed with the Olympus IX51 Inverted Microscope.

Western blotting

After 48 hrs of incubation, Vero cell monolayers infected at MOI of 0.1 were washed twice with PBS and resuspended in lysis buffer (50 mM Tris-HCl pH 7.5, 150 mM NaCl, 1 mM EDTA, 0.25% Triton X-100, 25 μg/ml PMSF, 50 μM leupeptin) at a concentration of approximately 5 x 10^6 cells/ml, considering the initial number of seeded cells before viral infection. Lysates were vortexed for 1 min and submitted to centrifugation at 12,000 g. The supernatants were collected and the concentration of protein determined by Qubit Protein Assay Kit (Life Technologies). The equivalent volume containing 20 ug of protein was mixed to the final 1x Laemmli buffer, supplemented with 5% of 2-mercaptoethanol. Samples were heated for 5 minutes at 95°C. Proteins in cellular extracts were then resolved by SDS-PAGE and subsequently transferred to PVDF membranes. Nonspecific sites on membranes were blocked with 5% nonfat milk in PBS-T (PBS pH 7.4, 0.1% Tween 20). Primary antibodies from mouse YF 17D polyclonal hyperimmune mouse ascitic fluid were diluted 1:2000 in 1% nonfat milk/PBST prior to incubation with membranes for 2 hrs at room temperature. The membranes were washed with PBST and incubated with secondary (goat α -rabbit HRP-conjugated, Amersham Biosciences) antibodies diluted 1:5000 in 1% nonfat milk/PBST for at least 1 hr at room temperature. Membranes were washed extensively with PBST and then developed with enhanced chemiluminescence (Amersham Biosciences) and autoradiography.

Animals and immunization protocols

Female BALB/c mice, 4–6 weeks old (CEMIB-UNICAMP, Campinas, São Paulo), were used in the YF 17D immunization studies. Groups of 5 mice were subcutaneously injected with two doses of cell culture media alone or 100,000 PFU of YF17D/SIV $Gag_{45\text{-}269}$, YF17D/SIV GagΔIRES or YF 17DD viruses with an interval of 15 days. Animal work was conducted in accordance with approved institutional animal ethics committee protocols (CEUA L-47/2011).

Plaque Reduction Neutralization Test (PRNT)

Four weeks after the last immunization, mice were bled by cardiac puncture. Serum sample treatment and YF neutralizing antibody titration were carried out by a method previously described (Bonaldo et al., 2007; Stefano et al., 1999). The values of neutralizing antibody titers of each experimental group were compared with the Kruskall Wallis test (GraphPad Prism 5.02 Program). The differences were considered significant when $P < 0.05$.

Antigenic sources

The YF 17DD virus adopted as an antigen during immunologic assays was obtained by cultivating the vaccine virus (MOI 1) in VERO cells until the appearance of the cytopathic effect. The infected-cell culture supernatant was clarified by centrifugation at 400 g for 15 min and aliquoted before storage at −80°C. The virus was titrated in triplicate. Inactivation was performed by heating at 56°C for 30 min. It has been already demonstrated that wild-type yellow fever virus, dengue virus, West Nile virus and hepatitis C virus (Fang et al., 2009; Song et al., 2010) are efficiently inactivated by this heating cycle regime. Since the

YF 17D virus was titrated prior to heat inactivation an equivalent MOI of 10 PFU/cell was applied.

A set of 60 peptides of 15 amino acids overlapping by 11 (15 x 11) and comprising the length between positions 41 and 291 of the SIVmac239 Gag protein, which encompass the entire Gag_{45-269} fragment was obtained from the NIH AIDS reagent program. The peptides were solubilized in DMSO and divided in pools of 10 peptides each, totaling 6 peptide pools called B, C, D, E, F and G, that match to the following Gag sequence intervals, 41–91, 81–131, 121–171, 161–211, 201–251 and 241–291, respectively.

IFN-γ ELISpot assay—For the IFN-γ ELISpot assay, groups of 5 mice, in each experiment, were immunized as described above. Fifteen days after the second immunization, the mice were sacrificed and the spleens removed. Splenocytes were isolated by standard methods as previously described (Nogueira et al., 2013). The results are presented after subtraction of the background and were compared adopting the Kruskall Wallis test with Dunn's post-test (GraphPad Prism 5.02 Program). The differences were considered significant when $P < 0.05$.

Intracellular cytokine staining (ICS)—Splenocytes from immunized mice were also assayed by ICS for interleukin 2 (IL-2) and IFN-γ. The cell suspensions, obtained as described above, were suspended to a final concentration of approximately 10^7 cells/ml. All groups of harvested spleen cells (1 X 10^6 cells / tube) were stimulated for 18 h with (1) medium alone, (2) whole heat-inactivated YF 17D virus, (3) pool of peptides described above or (4) concanavalin A (2 μg/ml; Sigma, St. Louis, MO) in the presence of 1 μg of anti-CD28 and anti-CD49d monoclonal antibodies/ml (BD PharMingen, San Diego, CA). Five hours before the end of the incubation, 10 μg/ml of brefeldin A (Sigma, St. Louis, MO) was added to each tube. Cells were then washed (PBS 10% FCS) and stained for surface antigens with PerCP anti-CD8 and Alexa 647 anti-CD4 mouse monoclonal antibodies (BD-Biosciences PharMingen, San Diego, CA). The cells were washed again, fixed with paraformaldehyde 2%, permeabilized (PBS 10% FCS 0,1% Saponin) and stained with monoclonal antibodies FITC anti-IL-2 and PE anti-IFN-γ (BD-Biosciences PharMingen, San Diego, CA) followed by multiparametric flow cytometry on FACScalibur flow cytometer using CellQuest software (BD Biosciences, San Jose, CA). The data were analyzed with FlowJo 7.6.5 for Windows software (Tree Star, Ashland, OR).

Supplementary Material

Refer to Web version on PubMed Central for supplementary material.

Acknowledgments

The authors are in debt to PDTIS-FIOCRUZ for supporting the sequencing, ELISpot and confocal microscopy studies through the Genomics, ELISpot and Confocal Microscopy Facilities. We are also grateful to Heloisa Diniz of Serviço de Produção e Tratamento de Imagem - IOC /FIOCRUZ and Marcia de Souza Santana for technical support with the figures presented in this work and to Richard Rudersdorf for technical assistance. This work was supported by grants from Fundação de Amparo à Pesquisa do Estado de Rio de Janeiro (Faperj), The National Institute for Vaccine Science and Technology (INCTV, MCT/CNPq), Conselho Nacional de Desenvolvimento Científico e Tecnológico (CNPq), Fiocruz and National Institutes of Health (NIH) HIVRAD grant 1P01AI094420 - 01A1.

English review and revision by Mitchell Raymond Lishon, native of Chicago, Illinois, U.S.A. – U.C.L.A. 1969.

References

Allen TM, Mothe BR, Sidney J, Jing P, Dzuris JL, Liebl ME, Vogel TU, O'Connor DH, Wang X, Wussow MC, Thomson JA, Altman JD, Watkins DI, Sette A. CD8(+) lymphocytes from simian immunodeficiency virus-infected rhesus macaques recognize 14 different epitopes bound by the major histocompatibility complex class I molecule mamu-A*01: implications for vaccine design and testing. Journal of virology. 2001; 75:738–749. [PubMed: 11134287]

Allen TM, Sidney J, del Guercio MF, Glickman RL, Lensmeyer GL, Wiebe DA, DeMars R, Pauza CD, Johnson RP, Sette A, Watkins DI. Characterization of the peptide binding motif of a rhesus MHC class I molecule (Mamu-A*01) that binds an immunodominant CTL epitope from simian immunodeficiency virus. Journal of immunology. 1998; 160:6062–6071.

Barba-Spaeth G, Longman RS, Albert ML, Rice CM. Live attenuated yellow fever 17D infects human DCs and allows for presentation of endogenous and recombinant T cell epitopes. The Journal of experimental medicine. 2005; 202:1179–1184. [PubMed: 16260489]

Bonaldo MC, Caufour PS, Freire MS, Galler R. The yellow fever 17D vaccine virus as a vector for the expression of foreign proteins: development of new live flavivirus vaccines. Memorias do Instituto Oswaldo Cruz. 2000; 95(Suppl 1):215–223. [PubMed: 11142718]

Bonaldo MC, Garratt RC, Caufour PS, Freire MS, Rodrigues MM, Nussenzweig RS, Galler R. Surface expression of an immunodominant malaria protein B cell epitope by yellow fever virus. Journal of molecular biology. 2002; 315:873–885. [PubMed: 11812154]

Bonaldo MC, Garratt RC, Marchevsky RS, Coutinho ES, Jabor AV, Almeida LF, Yamamura AM, Duarte AS, Oliveira PJ, Lizeu JO, Camacho LA, Freire MS, Galler R. Attenuation of recombinant yellow fever 17D viruses expressing foreign protein epitopes at the surface. Journal of virology. 2005; 79:8602–8613. [PubMed: 15956601]

Bonaldo MC, Martins MA, Rudersdorf R, Mudd PA, Sacha JB, Piaskowski SM, Costa Neves PC, Veloso de Santana MG, Vojnov L, Capuano S 3rd, Rakasz EG, Wilson NA, Fulkerson J, Sadoff JC, Watkins DI, Galler R. Recombinant yellow fever vaccine virus 17D expressing simian immunodeficiency virus SIVmac239 gag induces SIV-specific CD8+ T-cell responses in rhesus macaques. Journal of virology. 2010; 84:3699–3706. [PubMed: 20089645]

Bonaldo MC, Mello SM, Trindade GF, Rangel AA, Duarte AS, Oliveira PJ, Freire MS, Kubelka CF, Galler R. Construction and characterization of recombinant flaviviruses bearing insertions between E and NS1 genes. Virology journal. 2007; 4:115. [PubMed: 17971212]

Buck CB, Shen X, Egan MA, Pierson TC, Walker CM, Siliciano RF. The human immunodeficiency virus type 1 gag gene encodes an internal ribosome entry site. Journal of virology. 2001; 75:181–191. [PubMed: 11119587]

Castellino F, Germain RN. Cooperation between CD4+ and CD8+ T cells: when, where, and how. Annual review of immunology. 2006; 24:519–540.

Chambers TJ, Hahn CS, Galler R, Rice CM. Flavivirus genome organization, expression, and replication. Annual review of microbiology. 1990; 44:649–688.

Ciczora Y, Callens N, Seron K, Rouille Y, Dubuisson J. Identification of a dominant endoplasmic reticulum-retention signal in yellow fever virus pre-membrane protein. The Journal of general virology. 2010; 91:404–414. [PubMed: 19846669]

Darty K, Denise A, Ponty Y. VARNA: Interactive drawing and editing of the RNA secondary structure. Bioinformatics. 2009; 25:1974–1975. [PubMed: 19398448]

Deas TS, Binduga-Gajewska I, Tilgner M, Ren P, Stein DA, Moulton HM, Iversen PL, Kauffman EB, Kramer LD, Shi PY. Inhibition of flavivirus infections by antisense oligomers specifically suppressing viral translation and RNA replication. Journal of virology. 2005; 79:4599–4609. [PubMed: 15795246]

Fang Y, Brault AC, Reisen WK. Comparative thermostability of West Nile, St. Louis encephalitis, and western equine encephalomyelitis viruses during heat inactivation for serologic diagnostics. The American journal of tropical medicine and hygiene. 2009; 80:862–863. [PubMed: 19407138]

Franco D, Li W, Qing F, Stoyanov CT, Moran T, Rice CM, Ho DD. Evaluation of yellow fever virus 17D strain as a new vector for HIV-1 vaccine development. Vaccine. 2010; 28:5676–5685. [PubMed: 20600494]

Friebe P, Harris E. Interplay of RNA elements in the dengue virus 5′ and 3′ ends required for viral RNA replication. Journal of virology. 2010; 84:6103–6118. [PubMed: 20357095]

Gebhard LG, Filomatori CV, Gamarnik AV. Functional RNA elements in the dengue virus genome. Viruses. 2011; 3:1739–1756. [PubMed: 21994804]

Giraldo-Vela JP, Rudersdorf R, Chung C, Qi Y, Wallace LT, Bimber B, Borchardt GJ, Fisk DL, Glidden CE, Loffredo JT, Piaskowski SM, Furlott JR, Morales-Martinez JP, Wilson NA, Rehrauer WM, Lifson JD, Carrington M, Watkins DI. The major histocompatibility complex class II alleles Mamu-DRB1*1003 and -DRB1*0306 are enriched in a cohort of simian immunodeficiency virus-infected rhesus macaque elite controllers. Journal of virology. 2008; 82:859–870. [PubMed: 17989178]

Green DR, Ferguson T, Zitvogel L, Kroemer G. Immunogenic and tolerogenic cell death. Nature reviews Immunology. 2009; 9:353–363.

Herbreteau CH, Weill L, Decimo D, Prevot D, Darlix JL, Sargueil B, Ohlmann T. HIV-2 genomic RNA contains a novel type of IRES located downstream of its initiation codon. Nature structural & molecular biology. 2005; 12:1001–1007.

Hsieh SC, Tsai WY, Wang WK. The length of and nonhydrophobic residues in the transmembrane domain of dengue virus envelope protein are critical for its retention and assembly in the endoplasmic reticulum. Journal of virology. 2010; 84:4782–4797. [PubMed: 20181718]

Loffredo JT, Sidney J, Wojewoda C, Dodds E, Reynolds MR, Napoe G, Mothe BR, O'Connor DH, Wilson NA, Watkins DI, Sette A. Identification of seventeen new simian immunodeficiency virus-derived CD8+ T cell epitopes restricted by the high frequency molecule, Mamu-A*02, and potential escape from CTL recognition. Journal of immunology. 2004; 173:5064–5076.

Loffredo, JT.; Valentine, LE.; Watkins, DI. Beyond Mamu-A*01+ Indian Rhesus Macaques: Continued Discovery of New MHC Class I Molecules that Bind Epitopes from the Simian AIDS Viruses. In: Korber, BT.; Brander, C.; Haynes, BF.; Koup, R.; Moore, JP.; Walker, BD.; Watkins, DI., editors. HIV Molecular Immunology 2006/2007. Los Alamos National Laboratory; Los Alamos, New Mexico: 2007. p. 29-51.

Maciel M Jr, Kellathur SN, Chikhlikar P, Dhalia R, Sidney J, Sette A, August TJ, Marques ET Jr. Comprehensive analysis of T cell epitope discovery strategies using 17DD yellow fever virus structural proteins and BALB/c (H2d) mice model. Virology. 2008; 378:105–117. [PubMed: 18579176]

McAllister A, Arbetman AE, Mandl S, Pena-Rossi C, Andino R. Recombinant yellow fever viruses are effective therapeutic vaccines for treatment of murine experimental solid tumors and pulmonary metastases. Journal of virology. 2000; 74:9197–9205. [PubMed: 10982366]

Miller JD, Masopust D, Wherry EJ, Kaech S, Silvestri G, Ahmed R. Differentiation of CD8 T cells in response to acute and chronic viral infections: implications for HIV vaccine development. Current drug targets. Infectious disorders. 2005; 5:121–129. [PubMed: 15975018]

Monath, TP. Yellow fever vaccine. In: Plotkin, SA.; OWA; Offit, PA., editors. Vaccines. 4. WB Saunders; Philadelphia: 2004. p. 1095-1176.

Neves PC, Rudersdorf RA, Galler R, Bonaldo MC, de Santana MG, Mudd PA, Martins MA, Rakasz EG, Wilson NA, Watkins DI. CD8+ gamma-delta TCR+ and CD4+ T cells produce IFN-gamma at 5–7 days after yellow fever vaccination in Indian rhesus macaques, before the induction of classical antigen-specific T cell responses. Vaccine. 2010; 28:8183–8188. [PubMed: 20939995]

Nicholson MG, Rue SM, Clements JE, Barber SA. An internal ribosome entry site promotes translation of a novel SIV Pr55(Gag) isoform. Virology. 2006; 349:325–334. [PubMed: 16494914]

Nogueira RT, Nogueira AR, Pereira MC, Rodrigues MM, Neves PC, Galler R, Bonaldo MC. Recombinant yellow fever viruses elicit CD8+ T cell responses and protective immunity against Trypanosoma cruzi. PloS one. 2013; 8:e59347. [PubMed: 23527169]

Palmer DR, Fernandez S, Bisbing J, Peachman KK, Rao M, Barvir D, Gunther V, Burgess T, Kohno Y, Padmanabhan R, Sun W. Restricted replication and lysosomal trafficking of yellow fever 17D vaccine virus in human dendritic cells. The Journal of general virology. 2007; 88:148–156. [PubMed: 17170447]

Pierson TC, Diamond MS, Ahmed AA, Valentine LE, Davis CW, Samuel MA, Hanna SL, Puffer BA, Doms RW. An infectious West Nile virus that expresses a GFP reporter gene. Virology. 2005; 334:28–40. [PubMed: 15749120]

Pugachev KV, Guirakhoo F, Monath TP. New developments in flavivirus vaccines with special attention to yellow fever. Current opinion in infectious diseases. 2005; 18:387–394. [PubMed: 16148524]

Querec T, Bennouna S, Alkan S, Laouar Y, Gorden K, Flavell R, Akira S, Ahmed R, Pulendran B. Yellow fever vaccine YF-17D activates multiple dendritic cell subsets via TLR2, 7, 8, and 9 to stimulate polyvalent immunity. The Journal of experimental medicine. 2006; 203:413–424. [PubMed: 16461338]

Rice CM, Grakoui A, Galler R, Chambers TJ. Transcription of infectious yellow fever RNA from full-length cDNA templates produced by in vitro ligation. The New biologist. 1989; 1:285–296. [PubMed: 2487295]

Santos AP, Matos DC, Bertho AL, Mendonca SC, Marcovistz R. Detection of Th1/Th2 cytokine signatures in yellow fever 17DD first-time vaccinees through ELISpot assay. Cytokine. 2008; 42:152–155. [PubMed: 18378159]

Song H, Li J, Shi S, Yan L, Zhuang H, Li K. Thermal stability and inactivation of hepatitis C virus grown in cell culture. Virology journal. 2010; 7:40. [PubMed: 20167059]

Stefano I, Sato HK, Pannuti CS, Omoto TM, Mann G, Freire MS, Yamamura AM, Vasconcelos PF, Oselka GW, Weckx LW, Salgado MF, Noale LF, Souza VA. Recent immunization against measles does not interfere with the sero-response to yellow fever vaccine. Vaccine. 1999; 17:1042–1046. [PubMed: 10195613]

Tao D, Barba-Spaeth G, Rai U, Nussenzweig V, Rice CM, Nussenzweig RS. Yellow fever 17D as a vaccine vector for microbial CTL epitopes: protection in a rodent malaria model. The Journal of experimental medicine. 2005; 201:201–209. [PubMed: 15657290]

Todd DJ, Lee AH, Glimcher LH. The endoplasmic reticulum stress response in immunity and autoimmunity. Nature reviews Immunology. 2008; 8:663–674.

Trindade GF, Santana MG, Santos JR, Galler R, Bonaldo MC. Retention of a recombinant GFP protein expressed by the yellow fever 17D virus in the E/NS1 intergenic region in the endoplasmic reticulum. Memorias do Instituto Oswaldo Cruz. 2012; 107:262–272. [PubMed: 22415267]

Weill L, James L, Ulryck N, Chamond N, Herbreteau CH, Ohlmann T, Sargueil B. A new type of IRES within gag coding region recruits three initiation complexes on HIV-2 genomic RNA. Nucleic acids research. 2010; 38:1367–1381. [PubMed: 19969542]

Zou G, Xu HY, Qing M, Wang QY, Shi PY. Development and characterization of a stable luciferase dengue virus for high-throughput screening. Antiviral research. 2011; 91:11–19. [PubMed: 21575658]

Research Highlights

The YF 17D virus expressing part of the SIV Gag 45 to 269 protein fragment was genetically unstable;

The viral genetic stability was reached by mutating the IRES element localized in the *gag* gene fragment;

These genetic changes did not alter the rates of viral growth or immunogenicity in a mouse model.

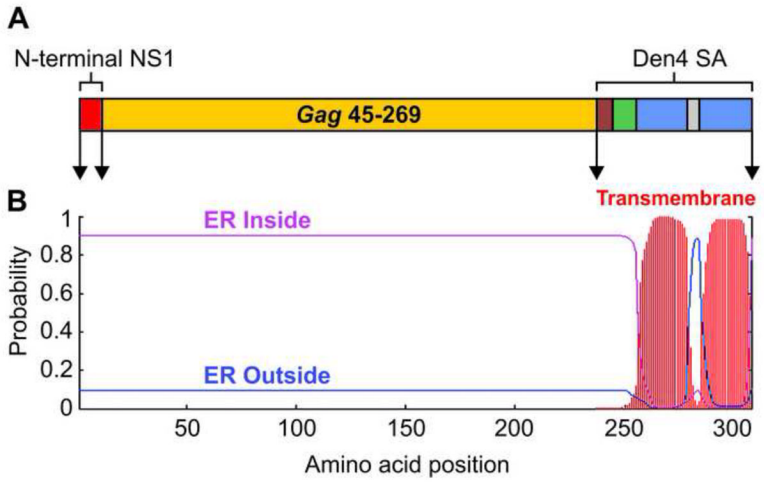

Figure 1.

Schematic diagram of the YF17D SIVmac239 $Gag_{45\text{-}269}$ expression cassette. (A) $Gag_{45\text{-}269}$ recombinant cassette fused at its 5′ and 3′ termini to YF motifs. The N-terminus of NS1 is shown in red. The C-terminus is made up of different components including the motif KESSIG (brown) and the truncated stem anchor domains of Dengue 4 virus E protein, the putative stem H2 motif (green) followed by the transmembrane domains T1 and T2 (blue). (B) Prediction plot of transmembrane helices in the $Gag_{45\text{-}269}$ cassette using the TMHMM Programm. The sequence was positioned inside or outside of endoplasmic reticulum (ER) based on the absence of transmembrane helices and the expected viral polyprotein topology.

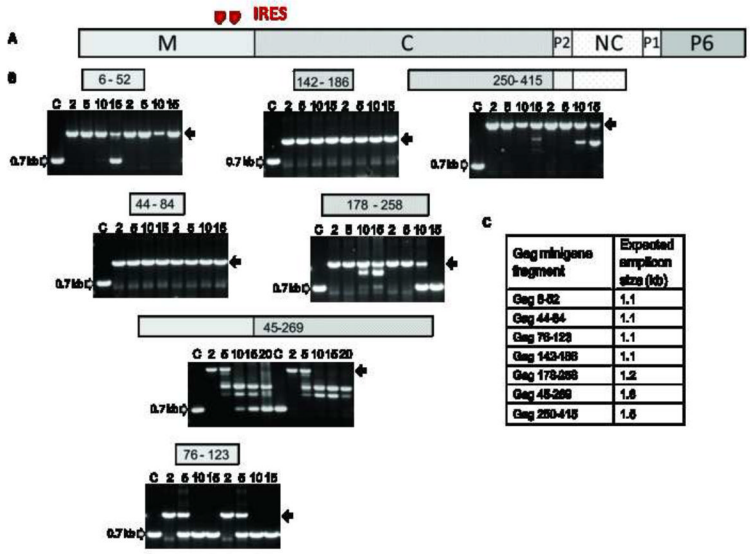

Figure 2.

Viral genetic stability studies performed in seven recombinant YF 17D viruses expressing different Gag fragments. (A) Organization of SIV *gag* gene coding Matrix (M), Capsid (C), Nucleocapsid (NC) proteins and the carboxy-terminal domain P6 as well as the spacer regions P1 and P2 (GenBank AY588946). (B) Electrophoretic analysis of amplicons containing the insertion region obtained by RT-PCR of viral RNA extracted from supernatant of cultures after serial passages in Vero cells. Numbers of passages are indicated above the figures. Grey arrows indicate the size of amplicons for viruses without insertion. Black arrows indicate the expected amplicon size for each recombinant virus containing the complete insertion. The corresponding Gag fragment that is expressed by each recombinant YF virus is specified above the electrophoretic profile. (C) Expected amplicon sizes for each recombinant virus.

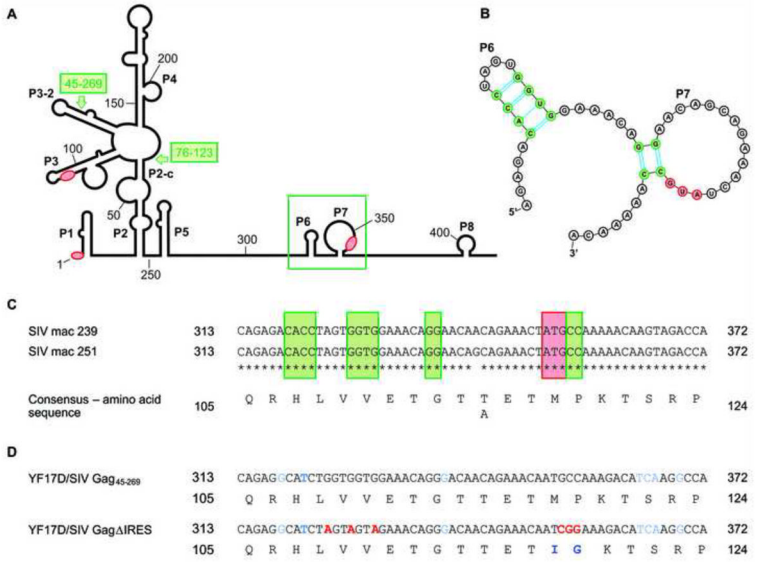

Figure 3.

Secondary structure model of the SIVmac239 5′ end of *gag* coding region, accordingly the model described by Weill et al., (2010). (A) The conserved structural elements forming pairings are designated P1 through P8. The three AUG in frame, initiation codons yielding three isoforms of the Gag, are indicated by red zones. Highlighted in a green box are indicated the elements P6 and P7 that were mutated in this work. The corresponding 5′ end of *gag* 45-269 and *gag 76-123* minigenes are indicated by green arrows and boxes. (B) Schematic drawing of the secondary structure of P6 and P7 RNA elements showing the nucleotides involved in pairing (green) as well as the AUG initiation code location (red) as illustrated by the VARNA program (Darty et al., 2009). (C) Alignment of SIVmac239 *gag* sequence containing the P6 and P7 elements with the corresponding sequence of SIVmac251 *gag* (GenBank AY588946) that was used to establish the structural model described elsewhere (Weill et al., 2010). (D) Alignment of the same *gag* regions present in YF17D/SIV $Gag_{45\text{-}269}$ and the mutated version virus YF17D/SIV GagΔIRES. The mutated nucleotides in YF infectious clone are shown in red. Nucleotide differences between the original SIV virus and recombinant YF17D/SIV viruses due to codon optimization are indicated in blue.

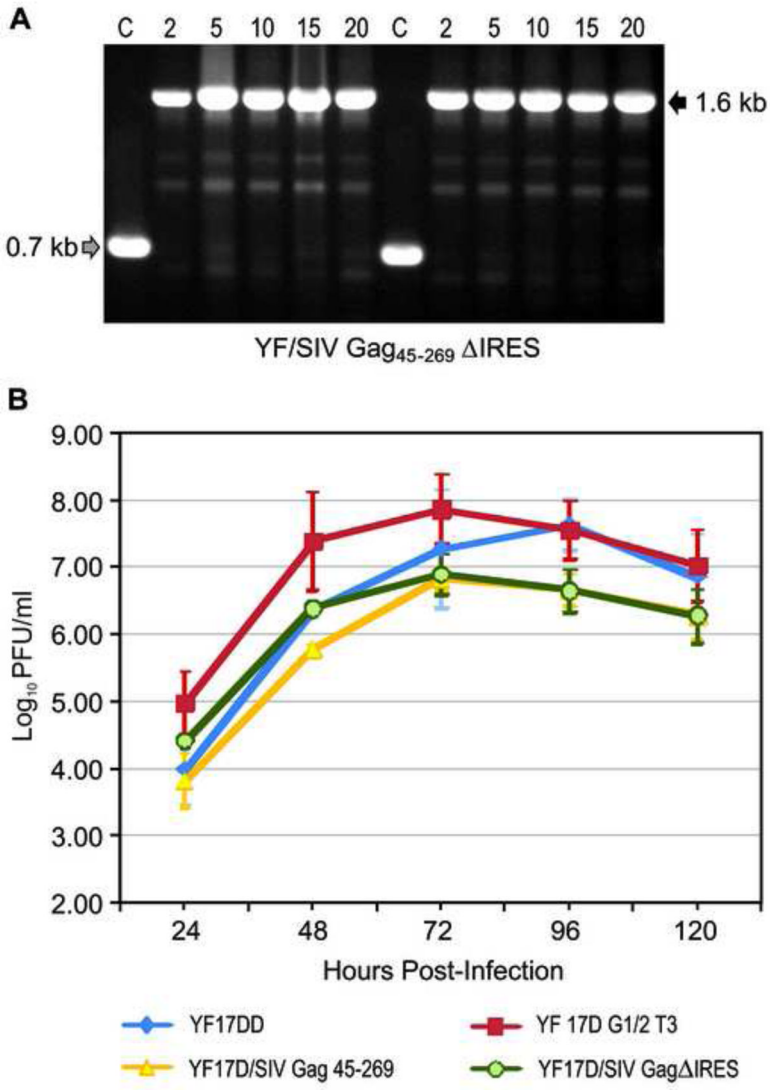

Figure 4.

Viral genetic stability and proliferation studies of the new recombinant YF17D/SIV GagΔIRES virus. (A) Electrophoretic analysis of amplicons containing the insertion region obtained by RT-PCR of viral RNA extracted from supernatant of cultures after serial passages in Vero cells. Numbers of passages are indicated above the figure. On the right, a black arrow indicates the size of the amplicon containing the complete heterologous expression cassette. On the left, the gray arrow points to the position of the YF 17D vaccine amplicon that does not contain any insertion. (B) Viral growth curves in Vero cells. Cells were infected with either the control YF 17DD (vaccine virus strain) and YF17D/G1/2T3 (parental clone) viruses or the recombinant YF17D/SIV $Gag_{45\text{-}269}$ or YF17D/SIV GagΔIRES viruses at MOI of 0.02. Each time point represents the average titer obtained from three independent experiments with the respective standard deviations.

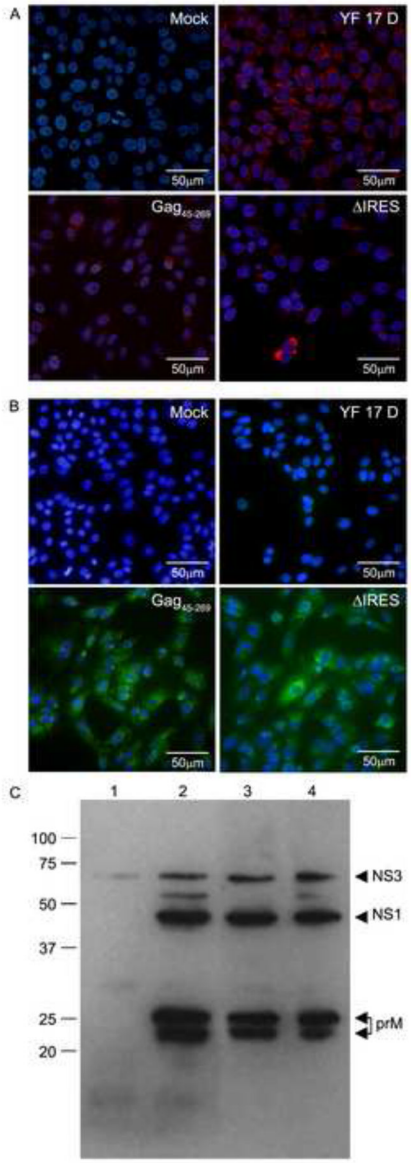

Figure 5.

Studies of the expression of the recombinant SIV $Gag_{45\text{-}269}$ protein by the recombinant YF/SIV $Gag_{45\text{-}269}$ viruses. Vero cells were viral infected with MOI of 0.1 and after 48 hr post-infection, cells were processed and stained with antibodies. (A) Immunofluorescence for intracellular detection of YF antigens in non-infected Vero cells monolayers (Mock) or cells infected with the YF 17D vaccine virus, the recombinant YF17D/SIV $Gag_{45\text{-}269}$ virus and YF17D/SIV GagΔIRES virus. (B) Intracellular detection of Gag antigen in Vero cells non-infected monolayers (Mock) or cells infected with YF 17D vaccine virus, the recombinant YF17D/SIV $Gag_{45\text{-}269}$ and YF17D/SIV GagΔIRES viruses. (C) Western blotting analysis for detection of YF proteins in lysates of Vero cells under denaturing conditions. Lanes: (1) Non-infected Vero cells lysates; (2) Lysates of Vero cells infected with YF 17DD virus; (3) YF17D/SIV $Gag_{45\text{-}269}$ virus; (4) YF17D/SIV GagΔIRES virus. Molecular weight markers are indicated on the right side of the membrane.

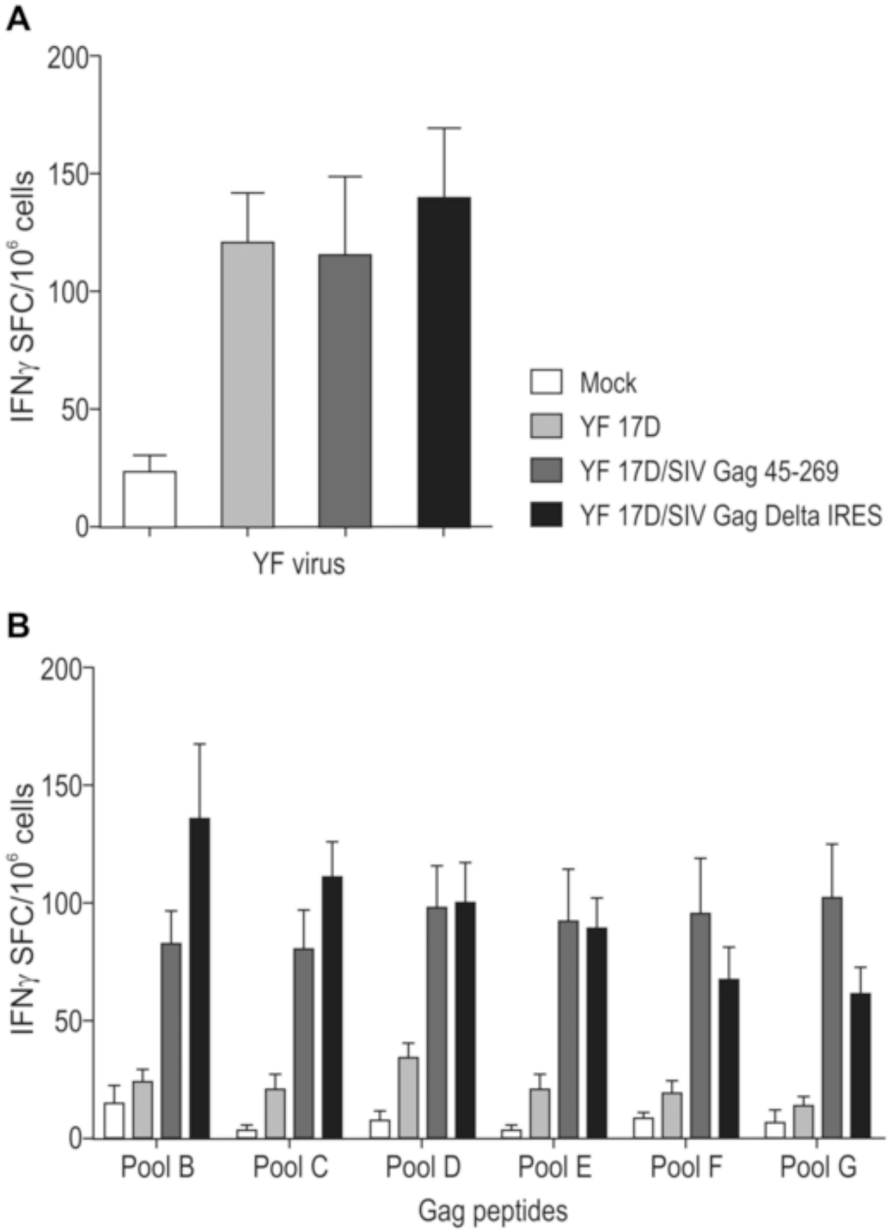

Figure 6.

ELISpot analysis of the induction of IFN-γ producing splenocytes after 14 days of mouse immunization. Groups of 5 mice were immunized twice with medium (mock), YF17 DD vaccine and the recombinant YF17D/SIV $Gag_{45\text{-}269}$ or YF17D/SIV GagΔIRES viruses. Spleen cells stimulated with heat-killed YF 17D virus (A) or with peptide pools corresponding to the inserted part of SIV-Gag protein. Data are representative of two independent experiments.

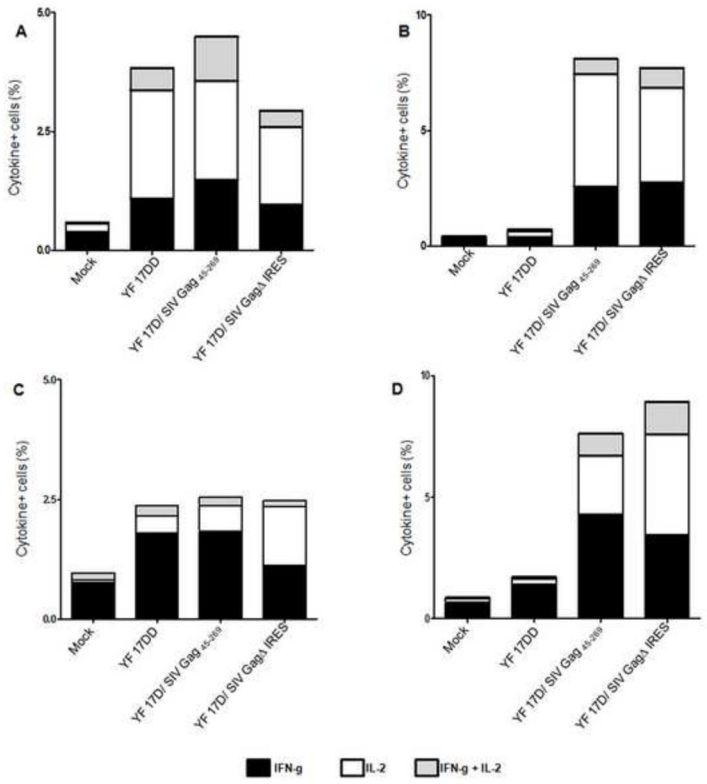

Figure 7.

Functional profile of CD4+ and CD8+ T cell responses in mice immunized with YF 17D and recombinant YF 17D viruses. We carried out multi-parameter ICS at day 14 after the second immunization to determine the ability of YF 17D and Gag specific splenocytes to secrete IFN-γ and/ or IL-2. The antigen stimuli in this assay consisted of whole inactivated YF 17DD virus or pools of SIVmac239 Gag peptides spanning the fragment Gag 45-269. Bar graphs indicate the average total frequency of IFN-γ+ (black), IL-2+ (white) or IFN-γ + IL-2+ (grey). (A) CD4+ T cells stimulated with YF 17DD virus, (B) CD4+ T cells stimulated with peptide pools of Gag, (C) CD8+ T cells stimulated with YF 17DD virus, (D) CD8+ T cells stimulated with peptide pools of Gag. The data were obtained from two independent experiments.

Table 1

Immunogenicity of the recombinant YF 17D viruses expressing Gag_{45-269} in BALB/c mice: titers of YF virus neutralizing antibodies after thirty days of the last dose.

			$PRNT_{50}$*	
Immunogen	**Animals (*n*)**	**% Sero-conversion to YF virus**	**GMT ± SD****	**Titer Range**
YF17DD	11	100	182 ± 89	27-1080
YF17D/SIV Gag_{45-269}	13	90	31 ± 6	14-84
YF17D/SIV GagΔIRES	11	100	30 ± 14	11-171
199 Earle's Medium	10	0	< 10	< 10

* values indicate the reciprocal of the dilution yielding 50% plaque reduction.

** Differences in the titers of neutralizing antibodies were statistically significant between 17DD immunized animals and YF17D/SIV Gag_{45-269} immunized animals ($p < 0.05$) as well as YF17D/SIV GagΔIRES virus ($P < 0.001$). Kruskal- Wallis with Dunn's post-test.